Millimeter-Wave Frequency Beam Scanning Array With a Phase Shifter Based on Substrate-Integrated-Waveguide

XIAOHE CHENG[1,2], (Student Member, IEEE), YUAN YAO[1], (Senior Member, IEEE),
TAKASHI TOMURA[2], (Member, IEEE), JIRO HIROKAWA[2], (Fellow, IEEE), TAO YU[2],
JUNSHENG YU[1], (Senior Member, IEEE), AND XIAODONG CHEN[3], (Fellow, IEEE)

[1]Beijing Key Laboratory of Work Safety Intelligent Monitoring, School of Electronic Engineering, Beijing University of Posts and Telecommunications, Beijing 100876, China
[2]Department of Electrical and Electronic Engineering, Tokyo Institute of Technology, Tokyo 152-8552, Japan
[3]School of Electronic Engineering and Computer Science, Queen Mary University of London, London E1 4NS, U.K.

Corresponding author: Yuan Yao (yaoy@bupt.edu.cn)

ABSTRACT In this paper, a millimeter-wave multi-folded frequency-dependent progressive phase shifter based on substrate-integrated-waveguide (SIW) is proposed. The equations based on SIW TE_{10} mode characteristic are applied to design the parameters of the phase shifter. An end-fire magneto-electric dipole with wide beam width is employed as the radiating element. By combining the antenna element and the phase shifter together, a frequency beam scanning antenna array is proposed and analyzed, using mathematical calculation based on phase array theory. A prototype of the proposed array has been fabricated and measured. The theoretical calculation of radiation pattern of the array is verified by full-wave electromagnetic solver Ansys HFSS and measurement. The measurement results show that the array can achieve a wide scanning range from $-18°$ to $32°$, gain variation less than 2.9 dBi, and radiation efficiency around 50% from 57 to 63 GHz. With the advantages of simple and compact structure, wide beam scanning range, and low-cost processing, the proposed array would be a good candidate for millimeter-wave wireless communication.

INDEX TERMS Frequency scanning array, millimeter-wave antenna, phase shifter, SIW.

I. INTRODUCTION

Frequency scanning antenna has been attracting great research interests due to its ability of beam-steering with the frequency variation and without any mechanical rotation or electrical adjustment. In recent years, with the development of millimeter-wave communication, which is regarded as a key solution for bandwidth expansion to address the exploding increase demand of data traffic in mobile communications, frequency scanning antenna has been employed in various millimeter-wave communication applications, such as WiGig (802.11.ad) systems [1] and base station antennas (BSA) in 5th-generation mobile networks (5G) [2]. And it has also been applied in millimeter-wave imaging system with a comparatively simple system complexity [3]. In terms of the antenna working principle, the frequency scanning antennas can be generally categorized into three types: quasi-optical feeding approach[4], series feeding with

open-ended structure [5], and full-corporate feeding with path difference phase shifter [6], [7].

The first type often employs the versatile quasi-optical approach and is ease of realizing high directivity and wide operating bandwidth performance in millimeter frequency band. In [8], a 3-D printed lens consisting of dielectric post elements was proposed to achieve frequency scanning beam around 275 GHz, where the phase difference for each element is realized by varying the height of the each dielectric post. But this kind of antennas is not suitable for compact applications due to its bulky structure. The second type employs leaky-wave principle as the main radiation mechanism, and thus has flexible broadside radiation directions, compact and simple structure. Many leaky-wave antennas based on SIW have been reported in [9]–[12].

The third type is a recently introduced method to achieve the frequency scanning beam with simple working principle.

Several works, which feed the frequency scanning antenna by the path difference phase shifter, have been reported in [6] and [7]. The requirement of frequency dependent progressive phase shift for each radiation element is achieved by using different length paths. A submillimeter-wave 2-D frequency scanning array composed of 8×8 open-ended air-filled metal waveguides and the path differences phase shifter was presented in [6]. Besides, for planarization design, eight identical slotted waveguides are used to replace the 2-D open-ended waveguide as the radiation element [7]. However, the spacing of the radiation elements is too large due to the width limit of air-filled waveguides, which increases the side-lobe level and requires more phase difference between adjacent radiation elements to obtain beam direction shifts. Furthermore, the open-ended waveguide has relatively narrow beam-width, which increases the gain variation for different direction beam.

Substrate integrated waveguide (SIW) is a type of low-cost and low-loss millimeter-wave transmission line and has a similar propagation property to the air-filled metal rectangular waveguide. Because it is designed on substrate with higher dielectric constant than air, the width of SIW is narrower than metal air-filled waveguide. Furthermore, multi-layer technologies for SIW have been reported in numerous research [13]–[16], which can achieved more compact size.

In this paper, a multi-folded phase shifter based on SIW is designed. Because the characteristic impedance of SIW is usually much lower than 377 Ω of free space, the open-ended structure cannot be treat as radiation element directly. For achieving better impedance matching and lower gain variation between different direction beams, an end-fire ME-dipole with wide beam width and impedance bandwidth is employed as radiation element. The phase difference of the frequency-dependent progressive phase shifter is analyzed by SIW TE_{10} mode characteristic, and the radiation pattern of the frequency beam scanning array is calculated by phase array theory. The full-wave electromagnetic solver Ansys HFSS and one processing example are employed to verify the analysis results.

The remaining parts of this paper are organized as follows. The operating principle and the structure of the SIW frequency-dependent progressive phase shifter are presented in Section II; the configuration and the simulation performance of the end-fire ME-dipole is given in Section III; Section IV describes the far field pattern of the theoretical analysis and the design procedure of the proposed array; Section V discusses the fabrication and measurement of one processing example. And in Section VI, the conclusions are summarized.

II. PHASE SHIFTER BASED ON SIW

The diagrams of the one-layer and multi-layer phase shifters are schematized in Fig. 1, comprising a four-way power divider and the different path distance transmission lines. The blue arrows represent the directions of the electromagnetic
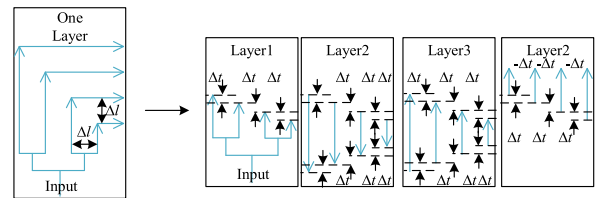

FIGURE 1. Layouts of the one-layer and multi-layer frequency-dependent progressive phase shifter.

wave propagation. The working mechanism of the phase shifter based on air-filled waveguide has been analyzed in [7]. Compared with one-layer structure, the multi-folded structure can significantly reduce the surface area. As shown in Fig. 1, the total path difference for adjacent outputs of the three-layer structure is $4\Delta t$. The diagram can be implemented in multi-layer SIW transmission line with slot coupling.
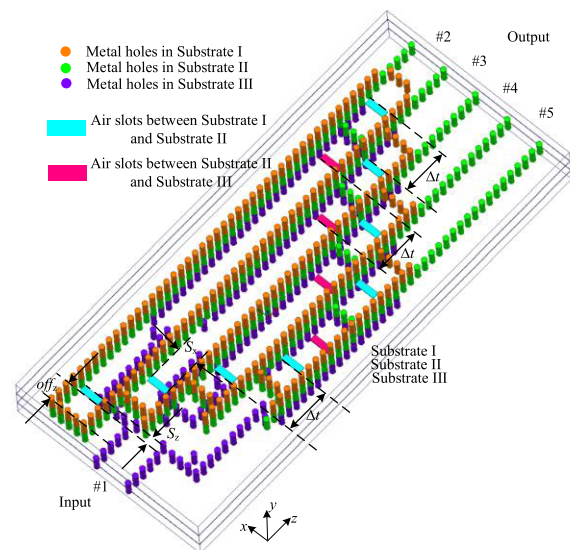

FIGURE 2. Configuration of the proposed multi-folded frequency-dependent progressive phase shifter based on SIW (the optimized values of dimensions of the phase shifter are listed in Table 1).

The three-layer SIW phase shifter corresponding to the diagram in Fig. 1 is shown in Fig. 2, which consists of one 1-4 power divider located at the bottom substrate (Substrate III) and three groups of coupling structure with path distance of Δt. In this design, all substrates are NPC-H220A (processed by Nippon Pillar Packing Co., Ltd.) with thickness of 1.2 mm, dielectric constant of 2.18 and dielectric loss tangent of 5×10^{-4}. All of the slots with length of S_x and width S_z are placed between the two laminate. The short-ended SIW sections with offset of off_z are placed in the adjacent substrates. It is important to obtain the accurate value of the adjacent distance of slot couplings Δt, due to the decisive effect on phase shifts.

The analysis of TE_{10} modes propagation characteristics can be transferred into the equivalent metal rectangular waveguide. The empirical relation between SIW

and conventional rectangular waveguide was proposed in [17],

$$w_{eff} = w - 1.08 \times \frac{d^2}{s} + 0.1 \times \frac{d^2}{w} \qquad (1)$$

where w is the width of the SIW, d represents the diameter of the metal holes and s denotes the spacing of adjacent metallic holes.

The operating wavelength of TE_{10} mode for SIW can be calculated by

$$\lambda_g = \frac{2\pi}{\sqrt{k^2 - \left(\frac{\pi}{w_{eff}}\right)^2}} \qquad (2)$$

where k is the wavenumber and can be calculated by

$$k = \frac{2\pi f \sqrt{\varepsilon_r}}{c} \qquad (3)$$

Then, the phase shift of the phase shifter can be obtained by

$$\Delta\alpha = 360 \times \frac{4\Delta t}{\lambda_g} \qquad (4)$$

where $4\Delta t$ is the path difference of adjacent outputs.

The theoretical calculation and full-wave electromagnetic simulation (solved by HFSS) of the SIW phase shifter with path distance of $\Delta t = 2.8$ mm, as shown in Fig. 2, are depicted in Fig. 3 with acceptable agreement. The simulated S-parameters and total loss of the phase shifter are presented in Fig. 4. The reflection coefficients are less than -14 dB and the transmission variations for each output port are less than 3.5 dB from 56 to 64 GHz. The total loss of the phase shifter can be obtained by

$$\alpha_{total} = 1 - S_{11} - S_{21} - S_{31} - S_{41} - S_{51} \qquad (5)$$

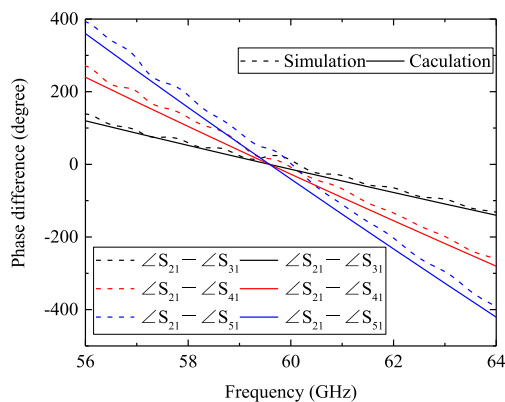where $S_{11}, S_{21}, S_{31}, S_{41}, S_{51}$ is presented in Fig. 4 (a).

FIGURE 3. The calculated and simulated phase differences of the proposed multi-folded frequency-dependent progressive phase shifter based on SIW.
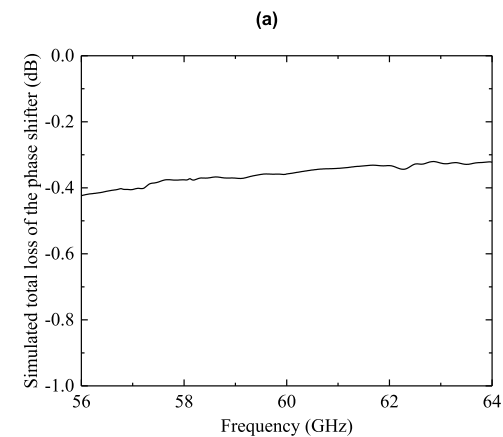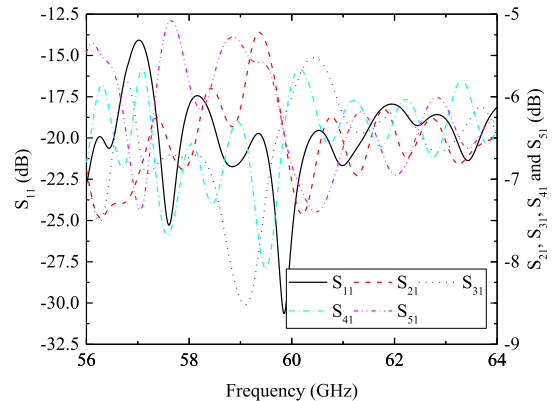

(a)

(b)

FIGURE 4. The simulated S-parameters and the total loss of the proposed multi-folded frequency-dependent progressive phase shifter based on SIW. (a) S-parameters. (b) loss.

TABLE 1. Dimension of the Phase Shifter (units: mm).

Parameters	Δt	S_x	S_z	*offz*
Values	2.8	1.56	0.49	2

III. ANTENNA ELEMENT

The antenna element of the scanning beam array with wide beam width has the advantage of smaller gain fluctuation for different direction beams, so that the ME-dipole is an attractive candidate for scanning beam array. The working principle and design procedure of the end-fire ME-dipole antenna has been proposed in [18]. In this design, the ME dipole is designed on three same NPC-H220A substrates with thickness of 1.2 mm as shown in Fig. 5. The positions of the metallic holes in substrate I and III are optimized to achieve the satisfactory radiation characteristics, such as stable gain, wide beam width and high front-to-back ratio. The open-ended SIW is designed in Substrate II. The optimized values of dimensions of the end-fire ME-dipole antenna are listed in Table 2.

The simulated reflection coefficients of the antenna elements are less than -13 dB from 56 to 64 GHz as presented
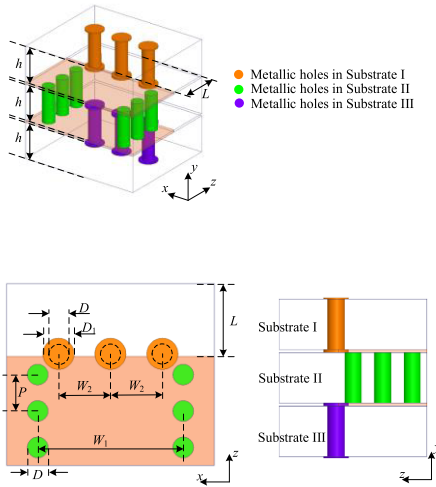
FIGURE 5. The structure of the ME-dipole element (the optimized values of dimensions of the phase shifter are listed in Table 2).

TABLE 2. Dimension of the antenna element (units: mm).

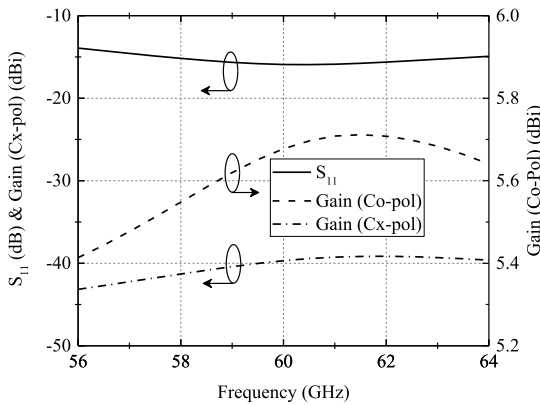| Parameters	h	W_1	W_2	P	D	D_1	L
Values	1.2	2.8	1	0.7	0.4	0.6	1.4

FIGURE 6. The S-parameter and gains of the ME-dipole element.

in Fig. 6. The primary polarization gains of 5.55 ± 0.15 dBi and cross polarization level less than -39 dBi are obtained. The simulated normalized radiation pattern in E- and H-plane at 57, 60 and 63 GHz are presented in Fig. 7. It can be seen that the half-power-beam-widths (HPBWs) in H-plane larger than 80° can be achieved.

IV. FREQUENCY BEAM SCANNING ARRAY
A. RADIATION PATTERN
By combining the antenna elements and the phase shifter together, the frequency beam scanning antenna array can be realized. Neglecting the mutual coupling of the radiation antenna elements, the radiation pattern of the one-dimensional array antenna $D(\theta, \varphi)$ can be expressed as the product of a vector element pattern $\mathbf{f}(\boldsymbol{\theta}, \boldsymbol{\varphi})$ and a scalar array
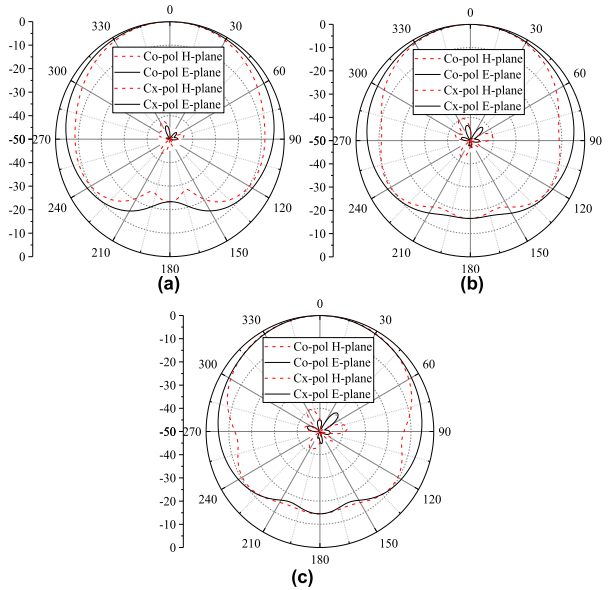

FIGURE 7. The radiation patterns of the ME-dipole element. (a) 57GHz. (b) 60 GHz. (c) 63GHz.

factor $F(\theta, \varphi)$,

$$D(\theta, \varphi) = \mathbf{f}(\boldsymbol{\theta}, \boldsymbol{\varphi}) F(\theta, \varphi) \tag{6}$$

Assuming that the geometrical center of the array aperture is located at the origin of the coordinate system, the antenna elements are arranged in the *x*-axis with spacing of W_1 and phase difference of $\Delta\alpha$ (calculated by Eq. (4)), the $F(\theta, \varphi)$ can be express as

$$F(\theta, \varphi) = \sum_{i=0}^{N-1} a_i e^{ji\Delta\alpha} e^{jk[(i-\frac{N-1}{2})W_1 \sin\theta \cos\varphi]} \tag{7}$$

Therefore, the normalized array factor for the four-elements array case can be calculated by

$$F(\theta, \varphi) = \cos\left(\frac{kw_1 \sin\theta + \Delta\alpha}{2}\right) \cos(kw_1 \sin\theta + \Delta\alpha) \tag{8}$$

The comparison between calculation and simulation results are given in Fig. 8.

B. DESIGN PROCEDURE
To serve as a guide for engineers, a simple stepwise procedure for designing the kind of the proposed frequency beam scanning is presented as follows.

Step 1: Based on the operating frequency band requirements, designing the width of SIW under the condition of main mode of TE$_{10}$ operation using Eq. (1).

Step 2: Fitting the beam directions for different frequency by using Eq. (7), the phase shift and element number can be obtained.

Step 3: Using Eq. (4) to obtain the path difference Δt.

*Step 4:* Correcting the theoretical error by optimized the path difference in full-wave simulation software.
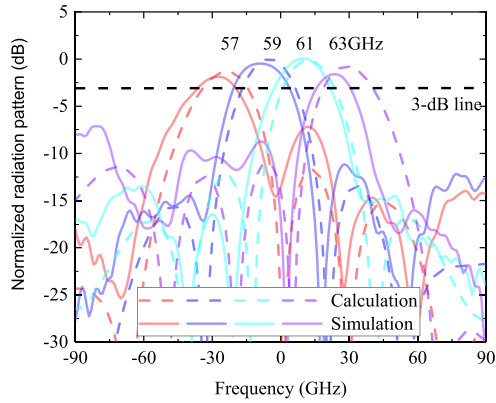
**FIGURE 8.** The calculated and simulated radiation patterns of the frequency beam scanning antenna array.

V. MEASUREMENTS

The photograph of the proposed frequency scanning array fabricated by traditional PCB facilities is given in Fig. 9. The simulated and measured normalized radiation patterns in *x-z* plane are illustrated in Fig. 10. The direction of the measured beam is shifted to right compared to simulations which is caused by the variation of dielectric constant of substrates. The main beams of measurements are coincided with simulations. The difference of the side lobe is mainly caused by the fabrication tolerance, such as increasing surface roughness caused by the scratches on the cladding, the cutting error of the radiating aperture of array and the inhomogeneity of the ring of radiation element, as shown in Fig. 9. These fabrication errors can be reduced to a very low level by using laser cutting technology of PCB facilities. The measured results show that the proposed array can achieve a beam scanning range from $-18°$ to $32°$ with side lobe level less than -5 dB from 57 to 63 GHz.
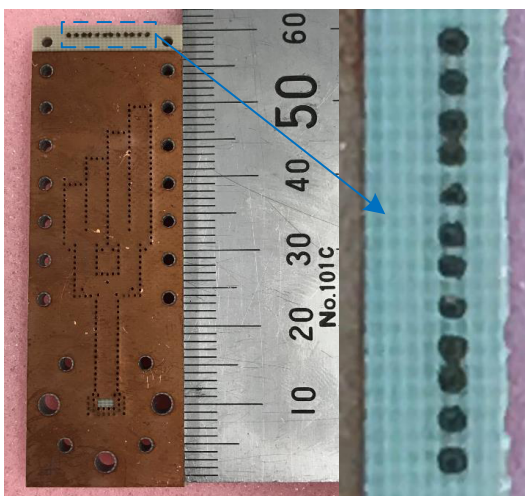

FIGURE 9. The prototype of the fabricated frequency beam scanning antenna array.

The simulated directivity and gain and measured gain of the proposed array are presented in Fig. 11. It should be noted that the reflection from the waveguide to SIW transitions have
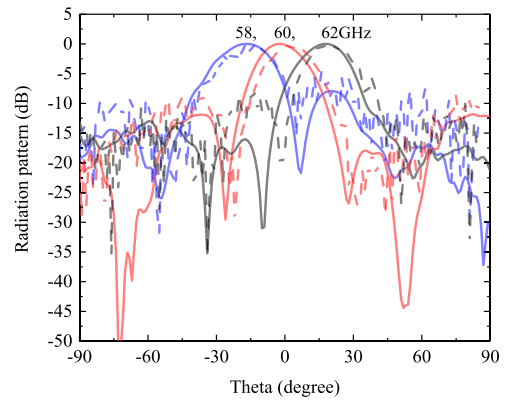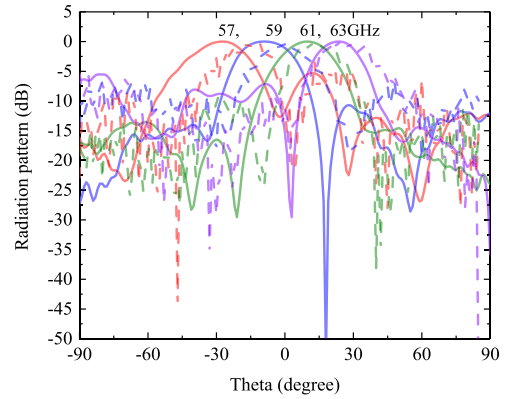
FIGURE 10. The simulated and measured radiation pattern of the frequency beam scanning antenna array.
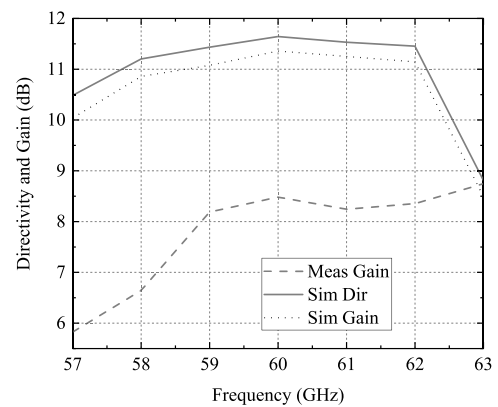
FIGURE 11. The simulated gain and directivity and measured gain of the frequency beam scanning antenna array.

been calibrated. The attenuation around 3 dB in measured results are mainly caused by the increasing surface roughness of cladding of stacked substrates in fabricated prototype [19]. The gain variations of each beam are less than 2.9 dBi. The radiation efficiency of the array is around 50%.

VI. CONCLUSION

A novel end-fire frequency beam scanning array based on SIW has been designed, fabricated and measured. To achieved the lower gain variations for different directional

beams, a ME-dipole with wide beam-width is employed as the radiating element. A three-folded frequency-dependent progressive phase shifter is used to feed the antenna elements. With the proposed mathematical formula, the radiation characteristics of the array can be obtained. A prototype was also fabricated and measured to validate the effectiveness of theoretical calculation and simulation. A 50° beam scanning range and gain variation less than 2.9 dBi can be achieved from 57 to 63 GHz.

REFERENCES

[1] Z. L. Ma, K. B. Ng, C. H. Chan, and L. J. Jiang, "A novel supercell-based dielectric grating dual-beam leaky-wave antenna for 60-GHz applications," *IEEE Trans. Antennas Propag.*, vol. 64, no. 12, pp. 5521–5526, Dec. 2016.

[2] F. M. Monavar, S. Shamsinejad, R. Mirzavand, J. Melzer, and P. Mousavi, "Beam-steering SIW leaky-wave subarray with flat-topped footprint for 5G applications," *IEEE Trans. Antennas Propag.*, vol. 65, no. 3, pp. 1108–1120, Mar. 2017.

[3] Y. Álvarez *et al.*, "Submillimeter-wave frequency scanning system for imaging applications," *IEEE Trans. Antennas Propag.*, vol. 61, no. 11, pp. 5689–5696, Nov. 2013.

[4] S. Li *et al.*, "Study of terahertz superresolution imaging scheme with real-time capability based on frequency scanning antenna," *IEEE Trans. THz Sci. Technol.*, vol. 6, no. 3, pp. 451–463, May 2016.

[5] Y. Li and J. Wang, "Dual-band leaky-wave antenna based on dual- mode composite microstrip line for microwave and millimeter-wave applications," *IEEE Trans. Antennas Propag.*, vol. 66, no. 4, pp. 1660–1668, Apr. 2018.

[6] R. Camblor, S. V. Hoeye, M. Fernández, C. V. Antuña, and F. Las-Heras, "Full 2-D submillimeter-wave frequency scanning array," *IEEE Trans. Antennas Propag.*, vol. 65, no. 9, pp. 4486–4494, Sep. 2017.

[7] R. Camblor, S. V. Hoeye, M. Fernández, C. V. A. Antuña, and F. Las-Heras, "Submillimeter wavelength 2-D frequency scanning antenna based on slotted waveguides fed through a phase shifting network," *IEEE Trans. Antennas Propag.*, vol. 65, no. 7, pp. 3501–3509, Jul. 2017.

[8] H. Yi, S.-W. Qu, K.-B. Ng, C. H. Chan, and X. Bai, "3-D printed millimeter-wave and terahertz lenses with fixed and frequency scanned beam," *IEEE Trans. Antennas Propag.*, vol. 64, no. 2, pp. 442–449, Feb. 2016.

[9] Y. L. Lyu *et al.*, "Leaky-wave antennas based on noncutoff substrate integrated waveguide supporting beam scanning from backward to forward," *IEEE Trans. Antennas Propag.*, vol. 64, no. 6, pp. 2155–2164, Jun. 2016.

[10] W. Zhou, J. Liu, and Y. Long, "Investigation of shorting vias for suppressing the open stopband in an SIW periodic leaky-wave structure," *IEEE Trans. Microw. Theory Techn.*, vol. 66, no. 6, pp. 2936–2945, Jun. 2018.

[11] K.-M. Mak, K.-K. So, H.-W. Lai, and K.-M. Luk, "A magnetoelectric dipole leaky-wave antenna for millimeter-wave application," *IEEE Trans. Antennas Propag.*, vol. 65, no. 12, pp. 6395–6402, Dec. 2017.

[12] C. S. Prasad and A. Biswas, "Dielectric image line-based leaky-wave antenna for wide range of beam scanning through broadside," *IEEE Trans. Antennas Propag.*, vol. 65, no. 8, pp. 4311–4315, Aug. 2017.

[13] Z. Chen, H. Liu, J. Yu, and X. Chen, "High gain, broadband and dual-polarized substrate integrated waveguide cavity-backed slot antenna array for 60 GHz band," *IEEE Access*, vol. 6, pp. 31012–31022, 2018.

[14] Y. Zhao and K.-M. Luk, "Dual circular-polarized SIW-fed high-gain scalable antenna array for 60 GHz applications," *IEEE Trans. Antennas Propag.*, vol. 66, no. 3, pp. 1288–1298, Mar. 2018.

[15] J. Wang, Y. Li, L. Ge, J. Wang, and K.-M. Luk, "A 60 GHz horizontally polarized magnetoelectric dipole antenna array with 2-D multi-beam endfire radiation," *IEEE Trans. Antennas Propag.*, vol. 65, no. 11, pp. 5837–5845, Nov. 2017.

[16] Q. Wu, J. Hirokawa, J. Yin, C. Yu, H. Wang, and W. Hong, "Millimeter-wave planar broadband circularly polarized antenna array using stacked curl elements," *IEEE Trans. Antennas Propag.*, vol. 65, no. 12, pp. 7052–7062, Dec. 2017.

[17] F. Xu and K. Wu, "Guided-wave and leakage characteristics of substrate integrated waveguide," *IEEE Trans. Microw. Theory Techn.*, vol. 53, no. 1, pp. 66–73, Jan. 2005.

[18] Y. Li and K.-M. Luk, "A multibeam end-fire magnetoelectric dipole antenna array for millimeter-wave applications," *IEEE Trans. Antennas Propag.*, vol. 64, no. 7, pp. 2894–2904, Jul. 2016.

[19] N. Bayat-Makou and A. A. Kishk, "Contactless air-filled substrate integrated waveguide," *IEEE Trans. Microw. Theory Techn.*, vol. 66, no. 6, pp. 2928–2935, Jun. 2018.

XIAOHE CHENG (S'17) received the B.Sc. degree from Hebei Univeirity, Baoding, China, in 2014. He is currently pursuing the Ph.D. degree in electronics and communication engineering with the Beijing University of Posts and Telecommunications, Beijing, China. Since 2017, he has been a Junior Visiting Fellow with the Ando and Hirokawa Laboratory, Tokyo Institute of Technology, Tokyo, Japan.

His current research interests include wideband antennas, circularly polarized antennas, and high-gain millimeter-wave antennas.

YUAN YAO (M'11–SM'15) received the B.Sc. degree in communication engineering from Tianjin University, China, in 2004, and the Ph.D. degree in electronic science and technology from Tsinghua University, China, in 2010.

In 2010, he joined the School of Electronic Engineering, Beijing University of Posts and Telecommunications, where he is currently a Full Professor. He has published over 100 papers and three books. His current research interests include the fields of antennas, RFID, and THz technology.

Dr. Yao is currently an Editor of the *International Journal of Antennas and Propagation* and also a Reviewer of the IEEE Transactions on Antennas and Propagation.
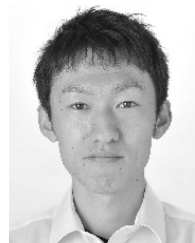
TAKASHI TOMURA (S'11–M'14) was born in Sendai, Japan. He received the B.S., M.S., and D.E. degrees in electrical and electronic engineering from the Tokyo Institute of Technology, Tokyo, Japan, in 2008, 2011, and 2014, respectively. He was a Research Fellow of the Japan Society for the Promotion of Science in 2013. From 2014 to 2017, he was at Mitsubishi Electric Corporation, Tokyo, where he was involved in research and development of aperture antennas for satellite communications and radar systems. He is currently a specially appointed Assistant Professor at the Tokyo Institute of Technology, Tokyo. His research interests include electromagnetic analysis, aperture antennas, and planar waveguide slot array antennas.

Dr. Tomura is a member of the IEICE. He received the Best Student Award from Ericsson Japan in 2012 and the IEEE AP-S Tokyo Chapter Young Engineer Award in 2015.

JIRO HIROKAWA (S'89–M'90–SM'03–F'12) received the B.S., M.S., and D.E. degrees in electrical and electronic engineering from the Tokyo Institute of Technology (Tokyo Tech), Tokyo, Japan, in 1988, 1990, and 1994, respectively.

He was a Research Associate from 1990 to 1996 and an Associate Professor from 1996 to 2015 at Tokyo Tech, where he is currently a Professor. He was with the antenna group of the Chalmers University of Technology, Gothenburg, Sweden, as a Post-Doctoral Fellow from 1994 to 1995. His research area has been in slotted waveguide array antennas and millimeter-wave antennas. He is a fellow of IEICE. He received IEEE AP-S Tokyo Chapter Young Engineer Award in 1991, the Young Engineer Award from IEICE in 1996, the Tokyo Tech Award for Challenging Research in 2003, the Young Scientists' Prize from the Minister of Education, Cultures, Sports, Science and Technology in Japan in 2005, the Best Paper Award in 2007, the Best Letter Award in 2009 from the IEICE Communications Society, and the IEICE Best Paper Award in 2016.

TAO YU received the B.E. degree in communication engineering from the Taiyuan Institute of Technology, China, in 2008, the M.E. degree in signal and information processing from the Communication University of China in 2010, and the Dr.Eng. degree from the Tokyo Institute of Technology in 2017. Since 2012, he has been with the Sakaguchi Laboratory, Department of Electrical and Electronic Engineering, Tokyo Institute of Technology, Japan, where he is currently a Post-Doctoral Researcher. His research interests are sensor networks, localization, distributed control, and building energy management. He is a member of IEICE.

JUNSHENG YU received the B.Sc. degree in physics from the Fuyang Teachers College, China, in 1983, the M.S. degree in physical electronics from the Southwestern Institute of Physics, China, in 1986, and the Ph.D. degree in electronic physics and devices from the University of Electronic Science and Technology of China, Chengdu, in 1990.

He received the Royal Society Scholarship in 1993 and did his visiting research in Abreu Thai Dundee University and the Imperial College University of London. In 2003, he joined the School of Electronic Engineering, Beijing University of Posts and Telecommunications, where he is currently a Full Professor. He has published dozens of papers. His research interests include microwave and millimeter wave theory, THz system, and physical electronics.

Dr. Yu is currently a member of experts group of the national high technology research and development program of China.
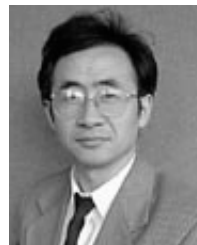
XIAODONG CHEN (M'96–SM'07–F'14) received the B.Sc. degree in electronic engineering from Zhejiang University, Hangzhou, China, in 1983, and the Ph.D. degree in microwave electronics from the University of Electronic Science and Technology of China, Chengdu, in 1988.

In 1988, he joined the Department of Electronic Engineering, King's College, University of London, as a Post-Doctoral Visiting Fellow. In 1990, he was with the King's College as a Research Associate and was appointed to an EEV Lectureship later on. In 1999, he joined the School of Electronic Engineering and Computer Science, Queen Mary University of London, where he is currently a Professor. He has authored and co-authored over 300 publications. His research interests include wireless communications, microwave devices, and antennas.

Dr. Chen is currently a member of the U.K. EPSRC Review College and the Technical Panel of the IET Antennas and Propagation Professional Network.

• • •